NASA Contractor Report 4064

Prediction of Recirculation Zones in Isothermal Coaxial Jet Flows Relevant to Combustors

M. Nallasamy

CONTRACT NAS8-35918
APRIL 1987

NASA

NASA Contractor Report 4064

Prediction of Recirculation Zones in Isothermal Coaxial Jet Flows Relevant to Combustors

M. Nallasamy
Universities Space Research Association
Boulder, Colorado

Prepared for
George C. Marshall Space Flight Center
under Contract NAS8-35918

National Aeronautics
and Space Administration

Scientific and Technical
Information Branch

1987

TABLE OF CONTENTS

PRECEDING PAGE BLANK NOT FILMED

LIST OF ILLUSTRATIONS

CONTRACT REPORT

PREDICTION OF RECIRCULATION ZONES IN ISOTHERMAL COAXIAL JET FLOWS RELEVANT TO COMBUSTORS

I. INTRODUCTION

The ever present demand for high power density engines for spacecrafts has resulted in engine designs that require the combustion system to operate at high pressure levels, higher fuel/oxidizer velocities, and increased outlet temperatures. The new design methodologies are greatly assisted by noninvasive Laser Doppler Anemometer (LDA) measurements in model combustors and advancement in combustion modeling resulting from the improvements in the numerics and computer memory and speed. One of the flow configurations often employed in modern combustors (for example, Space Shuttle) is that of coaxial jet flow. In this configuration, when the ratio of the velocity of the annular jet to that of the central jet is high, a large central toroidal recirculation zone (CTRZ) is formed in addition to the corner recirculation zone (CRZ) (Fig. 1). These two regions are the most important flow regions in any combustor flow field. Most of the combustion occurs in and near the recirculation zones. Maldistribution of high temperatures occurs in the practical combustor flow field, when the unburnt fuel escapes the recirculation zones and travels downstream. To correct maldistribution of high temperatures, details of the flow field and the means of controlling it should be known. The numerical simulation of the flow is now increasingly employed as a design tool for defining and understanding the combustor flow field [1-4].

The practical combustor flow field is turbulent, three-dimensional, multiphase, chemically reacting, and radiating. Numerical simulations consider the complex processes through appropriate simplified models [5,6]. The turbulence in the flow is taken care of by introducing closure models. The two equation, $k-\varepsilon$ model is often employed. In the currently available numerical simulation methods, models for chemical species calculation and radiation are particularly weak and need improvement [2]. A combination of idealized experiments, predictive methods and developments is helpful in making progress in numerical modeling. With this in mind, detailed experiments on two-dimensional axisymmetric flows have been carried out and reported in the literature for use in validating the mathematical models.

The coaxial jet flow is a complex one consisting of large recirculation zones whose occurrence depends on parameters such as the ratio of the velocities of the jets, ratio of the diameters of the jets, expansion ratio, inlet swirl, etc. Figure 1 shows the typical recirculation zones: (a) a corner recirculation zone which is present in most coaxial jet flow geometries and operating conditions with no inlet swirl; (b) a central toroidal recirculation zone whose formation in nonswirling flows depends mainly on the geometry and the velocity ratio. The numerical methods which model the coaxial jet flow need to predict these flow regions reasonably accurately, if the models are to be useful to the designer. The availability of reliable data for comparison with the calculation is a prerequisite for testing a numerical model. In an effort to provide such data and also to understand the nature of the flow in a coaxial jet flow configuration of interest to combustor designers, Owen [7] carried out detailed turbulence measurements using LDA.

Novick, et al. [8]; Syed and Sturgess [9]; and Sturgess, et al. [10] predicted the confined coaxial jet flow corresponding to the experimental conditions of Reference 7, employing the k-ε turbulence model. However, none of these predictions produced the shape, size, and location of the important central toroidal recirculation zone correctly. The length of the CTRZ was severely underpredicted by about 40 percent. Syed and Sturgess suspected that the central recirculation zone could extend into the central tube. Hence, Sturgess, et al. computed the flow starting from a section upstream of the expansion plane. This produced an apparent improvement in the predicted axial velocity on the centerline. But the shape, size and location of the CTRZ were incorrectly predicted compared to the measurements. Thus, so far no satisfactory prediction of the coaxial jet flow corresponding to the measurements of Reference 7 has been made. There is not even a speculation as to why the CTRZ is not well predicted. The present investigation was undertaken to study the characteristics of recirculation zones in coaxial jet flows in general, and in particular, to examine and improve the predictions corresponding to Owen's experiment.

II. THE PROBLEM

In coaxial jet flows with high velocity ratio, a central toroidal recirculation zone is formed due to the imbalance of the mass flow between the central and annular jets. The sudden expansion of the annular jet results in a severe (depending on the velocity ratio) adverse pressure gradient. When this pressure gradient is too strong for the low momentum central jet, a central toroidal recirculation zone results in addition to the corner recirculation zone (Fig. 1). The size and stability of these zones are important in combustors.

The factors that influence the size and stability of the recirculation zones are:

a) Details of the central jet exit configuration.

b) Velocity ratio, α = velocity of the annular jet, U_a/velocity of the central jet, U_p.

c) Magnitude of the velocities.

d) Expansion ratio, ER = diameter of the expansion chamber, D_e/diameter of the annular jet, D_o.

e) Diameter ratio of the jets, DR = diameter of the annular jet, D_o/ diameter of the inner jet, d_o.

f) Properties of the central and annular jet fluids.

For a fixed geometrical configuration, the velocity ratio and the magnitudes of the velocities are the factors that influence the recirculation zones. The aim of the present investigation is two-fold: First, to predict the coaxial jet flow corresponding to the experimental configuration of Owen [7]; second, to investigate the sensitivity of the recirculation zones to the details of central jet exit configuration, velocity ratio of the jets, and the magnitudes of velocities.

The Owen's experimental configuration (Fig. 2, reproduced here for clarity) consisted of a 2.5-in. (6.35-cm) central jet surrounded by a 3.5-in. (8.89-cm) annular jet. The jets discharge into a 5-in. (12.7-cm) diameter chamber 48-in. (121.9-cm) long. The outer and inner peak velocities were 96.0 (29.26) and 8.0 (2.44) fps (m/sec) corresponding to Reynolds numbers based on respective diameters of 1.5 and 0.08×10^5. No measured inflow profiles were reported.

III. THE NUMERICAL METHOD

Calculation of the confined coaxial jet flow field with large regions of recirculation requires the solution of the spatially elliptic form of the governing equations. The equations representing the conservation of mass, momentum, turbulence kinetic energy, and its rate of dissipation are represented in the general form

$$\mathrm{div}(\rho \vec{V} \phi) = \mathrm{div}(\Gamma_\phi \, \mathrm{grad}\, \phi) + S_\phi \tag{1}$$

where $\vec{V}$ is the velocity, ϕ is the fluctuating scalar quantity, Γ_ϕ is the diffusion coefficient of ϕ, S_ϕ is the source term for ϕ, and ρ is the fluid density. The equations are placed in discrete form by employing the finite volume method, and the resulting equations are solved numerically. The inlet section was located at a distance of 0.75 D_o upstream of the expansion plane. A fully developed flow was specified at the inlet. The inlet profiles for k and ε were specified in the usual manner [12]

$$k_{in} = 0.003\, U_{in}^{\;2} \tag{2}$$

$$\varepsilon_{in} = 0.09\, k_{in}^{1.5}/(0.03\, D/2) \quad . \tag{3}$$

The computational grid used for all the computations consisted of 40 x 40 nonuniformly distributed nodes, with a high gridline concentration in the separated layer and near the walls. The grid extended to an axial distance of 11.25 D_o. Tests showed that this nonuniform grid produced nearly mesh independent (with little change in the sizes of the recirculation zones) solution. All the computations have been performed by means of PHOENICS computer program of Spalding [13]. One of the very useful concepts adopted in this program is that of "porosity" to modify the regular grid cells. Irregular geometry and blockages in the flow field can be conveniently represented using the grid porosity. This is done by specifying a set of factors which will multiply the areas/volumes associated with the grid, which has been nominally set up. In the present computation, partially or fully blocked grid cells were represented using porosity.

IV. DISCUSSION OF RESULTS

First, the predictions of the flow field corresponding to the experimental conditions of Owen [7] are described. Then, the sensitivity of the recirculating zones to different controlling parameters is discussed.

A. Predictions of the Flow Field for Owen's Experimental Configuration

The coaxial jet flow patterns corresponding to Owen's experimental conditions predicted by Novic, et al. [8] and Sturgess, et al. [10] are reproduced here in Figures 3(a) and 3(b), respectively, for comparison. A comparison of these with the experimental flow pattern [Fig. 3(d)] shows clearly that the location, shape, and size of the central toroidal recirculation zone are not predicted satisfactorily. Examinations of these predictions and the schematic of the experimental arrangement in Figure 2 gave the clue as to why these predictions do not predict the flow field correctly. The important points to note are: (a) the central jet wall does not end at the expansion plane, and (b) the central jet (pipe) wall is chamfered outward. These important details were not incorporated in the above predictions. When these two factors are taken into account in the definition of the geometry using the porosity concept of the PHOENICS computer program, the location, shape and size of the recirculation zones are correctly predicted as shown in Figure 3(c). Thus, for the first time, the flow field corresponding to Owen's experiment is predicted satisfactorily. In what follows, a physical explanation of the processes leading to the formation of recirculation zones of observed sizes is given and then, detailed comparisons of the predictions with measurements are presented.

For the velocity ratio (=12) considered here, the growth of the mixing layers emanating from the tips of the inner and outer jet walls is essentially controlled by the outer jet. When the inner jet wall ends at the expansion plane, the (virtual) origin of the inner mixing layer may be assumed at this point, O_1. That is, the origins of both inner and outer mixing layers are at the expansion plane. Then, the spread of the two mixing layers is about the same, thus resulting in the same value for the lengths of the corner and central recirculation zones (Fig. 4). This is the result observed in earlier predictions of the flow [8,10], as well as in the present study of this configuration [Fig. 5(c)]. However, for the configuration of the experiment, the origin of the inner mixing layer is shifted downstream to O_2, while the origin of the outer mixing layer remains unchanged. The spread rate of the inner mixing layer is about the same as before (except for the modification due to the interactions of the two mixing layers). This results in a longer central recirculation zone as shown in the figure. The length of the corner recirculation zone is reduced because of the stabilizing effect of the extending central jet wall. This is similar to the stabilizing effect in the asymmetric channel expansion-flow over a backward facing step, where the length of the recirculation zone is smaller compared to the symmetric channel expansion [12]. These two processes result in the observed shape, size and location of the recirculation zones.

The centerline mean axial velocities obtained in the present prediction and experiment are shown in Figure 5. The agreement between the two is good up to a distance of 2.25 D_o. Beyond this the predicted value is smaller than the measured one. This is due to the slow development of the flow beyond the reattachment of the dividing streamline on the centerline. The slow redevelopment of the flow has been observed in most of the k-ε model predictions of recirculating flows [14,15]. The observed redevelopment is due to the inability of the k-ε model to correctly represent this region, where the flow is changing from the separated to reattached one. It is not characteristic of either a boundary layer or a free-shear layer. The axial turbulence intensity on the centerline is shown in Figure 6. The agreement with the measurements is very good up to an axial distance of 1.75 D_o. Beyond this, the turbulence intensity falls more quickly than in the experiment. This appears to be due to the incorrect representation of the redevelopment of the flow in the model. However, the general shape of the profile is correctly predicted.

Figure 7 shows the radial profiles of the mean axial velocity at two axial locations, $X = 0.36\ D_o$ and $1.43\ D_o$. The predicted velocity profiles are in reasonably good agreement with the measurement. The maximum discrepancies observed are in the region of maximum shear. Mean radial velocity profiles at the two downstream sections are shown in Figure 8. At the section near the jet exit ($X = 0.36\ D_o$), the computation shows a negative radial velocity region near the expansion chamber wall. No experimental points have been shown in this region (the line drawn through the experimental points shows no negative velocities [7]). The negative radial velocity observed in the prediction is to be expected, due to the corner recirculation zone, and no velocity components were measured in this zone. At the downstream section ($X = 1.43\ D_o$), the predicted velocities are in reasonable agreement with measurements. The maximum discrepancy occurs in the wake region of the jet wall, at both axial stations. This is in accordance with the observations of Pope and Whitelaw [16].

The detailed comparisons of axial and radial mean velocities, turbulence intensities and recirculation zones presented show that the present computations produce the coaxial jet flow field reasonably accurately. In combustor design, the central jet exit geometry is designed to establish the required flame length and stability. The sensitivity of the recirculation zones to the central jet exit geometry is presented below.

B. Effects of Central Jet Exit Configuration

The central jet exit geometrical configuration is designed according to the requirements of flame length (recirculation zone length) and stability. Five different configurations of the central jet exit geometry and the predicted recirculation zone boundaries for each case are shown in Figure 9. The loci of the flow reversals ($\bar{U} = 0$) have been plotted for the corner and central recirculation zones. The longitudinal extent of these regions are in accordance with the expectations based on Figure 4. Thus, the effects of central jet exit geometry are qualitatively well predicted in the present computations (no experimental data are available for direct comparison). A configuration similar to that shown in Figure 9(a) is employed in Space Shuttle Main Engine injector elements to introduce fuel and oxidizer into the preburners and the main combustion chamber. In this case, the central recirculation zone starts well before the expansion plane. In Figure 9(b), the blunt edge of the central jet wall pushes the central recirculation zone a little downstream (due to a thicker wake region) and increases the length of the corner recirculation zone. The configuration studied by Novic, et al. [8] and Sturgess, et al. [10] is shown in Figure 9(c). In this case, since the two mixing layers grow from the same section (expansion plane), the shape of the central recirculation zone is quite different from those of Figures 9(a) and 9(b). The length of the two recirculation zones (CRZ and CTRZ) are almost the same, as observed in the previous investigations. Figure 9(d) shows the recirculation zones for the case where the central pipe wall extends beyond the expansion plane. This produces the location, shape and size of the recirculation zones very close to the experimentally observed ones. We see here that the length of the corner recirculation zone is decreased for the reasons explained above (Fig. 4). However, only when the pipe edge is chamfered as in the experimental configuration

[Fig. 9(e)], the size, shape and location of CRZ and CTRZ are in agreement with those of the measurements [also Fig. 3(c)]. Thus, it is shown that the sensitivity of the recirculation zones to the central jet exit geometry can be correctly predicted by the numerical solution. This can aid the designer in selecting the configuration of the central jet exit geometry.

The observed changes in the characteristics of the recirculation zones with the pipe wall exit geometry should result in significant differences in wall static pressure beyond the expansion plane. Figure 10 shows the wall static pressure variation corresponding to the configurations of Figures 9(a), 9(c), and 9 (e). Only these cases are shown for clarity. The pressure recovery is faster for the configuration in Figure 9(a) where the length of the CRZ is small and CTRZ starts well before the expansion plane. For the case in Figure 9(c) the recovery is much slower as CRZ is longer. For the experimental configuration in Figure 9 (e), the wall static pressure variation is quite different from the other two. The initial recovery is faster since the length of CRZ is small as in Figure 9(a). But the pressure coefficient drops again due to the growth of the width of the CTRZ even beyond the extent of CRZ. The wall static pressure in the expansion chamber is thus very sensitive to the central jet exit geometry.

C. Effect of Velocity Ratio

It was shown that for the experimental conditions of Owen, the flow field can be predicted reasonably well. For the same geometrical configuration, the effect of velocity ratio on the recirculation zones is examined. The central toroidal recirculation boundaries for four velocity ratios, namely 12, 9, 6, and 3 are shown in Figure 11. No CTRZ is formed for a velocity ratio of 2 or 1. With the reduction in velocity ratio from 12 to 6, the distance of the CTRZ from the expansion plane increases — the separation bubble moves downstream gradually. However, for a velocity ratio of 3 the CTRZ is pushed far downstream.

The observed behavior of the CTRZ with the velocity ratio may be understood from the mixing layer characteristics. Figure 12 shows the growth rate of the thickness of a two-stream mixing layer plotted against the velocity difference parameter, λ (adopted from Brown and Roshko [17]). If U_1 and U_2 are the velocities of the two streams, then λ is defined as $\lambda = (U_1-U_2)/(U_1+U_2)$. As the velocity ratio is decreased from 12 to 6, the growth rate of the mixing layer decreases gradually, since λ decreases gradually. The smaller the growth rate the farther the separation bubble moves from the expansion plane. But for a velocity ratio of 3, λ becomes 0.5 for which the growth rate differs significantly from that for 6. This means slow development of the mixing layer and it is reflected in the movement of CTRZ far downstream for $\alpha = 3$. For a velocity ratio of 2 the growth rate is small and the adverse pressure gradient is not strong enough to produce a CTRZ. It is interesting to note that the length of the CTRZ does not change significantly when the velocity ratio increases from 3 to 12.

The maximum return flow velocity in the CTRZ increases with increase in velocity ratio, α (Fig. 13). It is seen that the maximum return flow velocity (occurring on the centerline) is nearly proportional to the strength (U_a-U_p) of the mixing layer.

The characteristics of the corner recirculation zone is more complicated by the confining wall and the interaction of the two mixing layers. The variation of the length of the corner recirculation zone with velocity ratio is shown in Figure 14. The increase in the length of CRZ is gradual with the decrease of the velocity ratio up to 3. For $\alpha = 2$, with no CTRZ, the length of CRZ increases sharply. With a velocity ratio of unity, the flow resembles that of a simple pipe expansion flow and has a longer corner recirculation zone. The length is now 7.7 H, where H is the step height equal to $(D_e - D_o)/2$. For a simple pipe expansion of the same expansion ratio, the length of CRZ was obtained as 8.7 H by Moon and Rudinger [18]. The pipe wall extending beyond the expansion plane [Fig. 5(e)] is responsible for the lower value of 7.7 H as explained above. With pipe wall ending at the expansion plane [Fig. 5(c)] the length of CRZ is obtained as 8.5 H (shown in the figure by the point ⊡). It is instructive to note that Habib and Whitelaw [14] observe an increase in the length of CRZ when the velocity ratio is increased from 1 to 3, in contrast to the present results. However, it should be noted that for $\alpha = 3$, they do not observe any CTRZ for their geometry (expansion ratio of 2.81 and diameter ratio of 2.76). Johnson and Bennet [19] also do not find a CTRZ for $\alpha = 3.11$ for their geometry (expansion ratio of 2.07 and diameter ratio of 1.93).

D. Effect of Reynolds Number

The growth of the mixing layer emanating from the tip of the inner jet wall is dependent on a single parameter λ, as in any mixing layer [17]. If λ is held constant, then the growth rate is constant. In other words the diffusion process is essentially controlled by this paraemter. If the Reynolds numbers of the two jets are increased while keeping λ constant, the recirculation lengths should be invariant. This was verified in the computation by increasing the Reynolds number of the inner and outer jets by four- and eight-folds. The parameter λ was kept constant equal to 0.846 for a velocity ratio of 12. The calculations showed that the corner recirculation zone remained essentially constant. The central recirculation zone length varied by about 0.1 D_o which is about 7 percent. This probably represents the error introduced by using the same grid layout for high Reynolds number computations. It is instructive to note that for a simple pipe expansion flow, the length of the recirculation zone becomes independent of Reynolds number, in the computations, only beyond $Re = 10^5$ [20] on a similar grid layout (42 x 42).

V. CONCLUSIONS

1) In a coaxial jet flow, the corner and central recirculation zones are very sensitive to the central jet exit geometry. The numerical solution can predict them reasonably accurately.

2) For a given geometrical configuration, the velocity ratio determines the axial location of the central toroidal recirculation zone.

3) For the geometrical configuration studied, the length of the corner recirculation decreases with increase in velocity ratio in contrast to the results of Habib and Whitelaw.

4) For a velocity ratio of 3, the experimental configuration of Owen results in the formation of CTRZ while the configurations of Habib and Whitelaw and Johnson and Bennet produce no CTRZ.

5) The k-ε turbulence model predicts the location, shape and size of the recirculation zones fairly well. In these regions, the predicted axial and radial mean velocities and axial turbulence intensity are in good agreement with the measurements. However, the redevelopment of the flow beyond the reattachment on the centerline is slow compared to the measurements.

REFERENCES

1. Gupta, A. K., Lilley, D. G., and Syred, N.: Swirl Flows. ABACUS Press, 1984.

2. Lefebvre, A. H. (Ed.): Gas Turbine Combustor Design Problems. Hemisphere, 1980.

3. Jones, W. P. and Whitelaw, J. H.: Calculation Methods for Reacting Turbulent Flows: A Review. Combustion and Flame, Vol. 48, 1982, pp. 1-26.

4. Drummond, J. P.: Numerical Study of a Ramjet Dump Combustor Flow Field. AIAA Journal, Vol. 23, 1985, pp. 604-611.

5. Boyson, F., Ayers, W. H., Swithenbank, J., and Pan, Z.: Three Dimensional Model of Spray Combustion in Gas Turbine Combustors. Journal of Energy, Vol. 6, 1982, pp. 368-375.

6. Swithenbank, J., Turan, A., and Felton, P. G.: Three Dimensional Two-phase Mathematical Modeling of Gas Turbine Combustors. Project SQUID, Gas Turbine Combustor Design Problems, Purdue University, 1978.

7. Owen, F. K.: Measurement and Observations of Turbulent Recirculating Jet Flows. AIAA Journal, Vol. 14, 1976, pp. 1556-1562.

8. Novic, A. S., Miles, G. A., and Lilley, D. G.: Numerical Simulation of Combustor Flow Fields: A Primitive Variable Design Capability. Journal of Energy, Vol. 3, 1979, pp. 95-105.

9. Syed, S. A. and Sturgess, G. A.: Validation Studies of Turbulence and Combustion Models for Aircraft Gas Turbine Combustors. In: Momentum and Heat Transfer Process in Recirculating Flows, HTD-Vol. 13, 1980, pp. 71-89.

10. Sturgess, G. J., Syed, S. A. and McManus, K. R.: Importance of Inlet Boundary Conditions for Numerical Simulation of Combustor Flows. AIAA Paper No. AIAA-83-1263, 1983.

11. Launder, B. E. and Spalding, D. B.: The Numerical Computation of Turbulent Flows. Computational Methods in Applied Mechanics and Engineering, Vol. 3, 1974, pp. 269-289.

12. Nallasamy, M.: A Critical Evaluation of Various Turbulence Models as Applied to Internal Fluid Flows. NASA Technical Paper 2474, 1985.

13. Spalding, D. B.: A General Purpose Computer Program for Multidimensional Two-phase Flow. In: Mathematics and Computers in Simulation, Vol. XIII, 1981, pp. 267-276.

14. Habib, M. A. and Whitelaw, J. H.: Velocity Characteristics of a Confined Coaxial Jet. Journal of Fluids Engineering, Vol. 101, 1979, pp. 521-529.

15. Habib, M. A. and Whitelaw, J. H.: Velocity Characteristics of Confined Coaxial Jets With and Without Swirl. Journal of Fluids Engineering, Vol. 102, 1980, pp. 47-53.

16. Pope, S. B. and Whitelaw, J. H.: The Calculation of Near Wake Flows. Journal of Fluid Mechanics, Vol. 73, 1976, pp. 9-32.

17. Brown, G. L. and Roshko, A.: On Density Effects and Large Structures in Turbulent Mixing Layers. Journal of Fluid Mechanics, Vol. 64, 1974, pp. 775-816.

18. Moon, L. F. and Rudinger, G.: Velocity Distribution in an Abruptly Expanding Circular Duct. Journal of Fluids Engineering, Vol. 99, 1977, pp. 226-230.

19. Johnson, B. V. and Bennet, J. C.: Mass and Momentum Transport Experiments with Confined Coaxial Jets. NASA CR-165574, 1981.

20. Nallasamy, M. and Chen, C. P.: Studies on Effects of Boundary Conditions in Confined Turbulent Flow Predictions. NASA CR-3929, 1985.

ORIGINAL PAGE IS OF POOR QUALITY

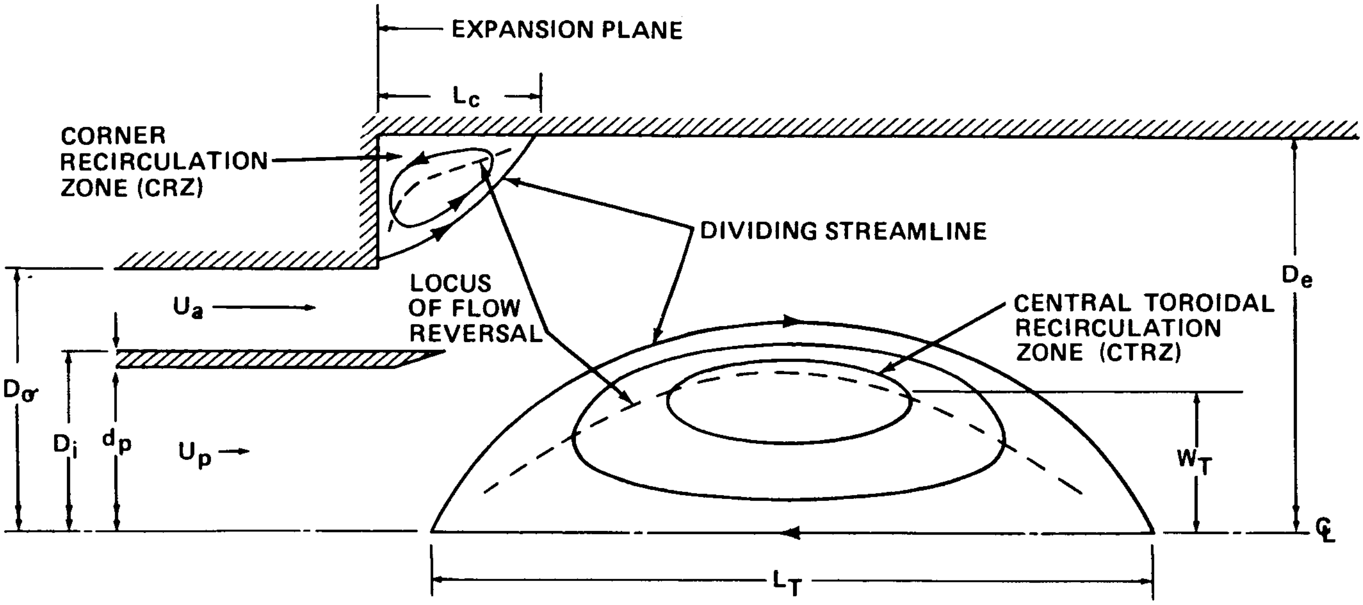

Figure 1. Definition sketch.

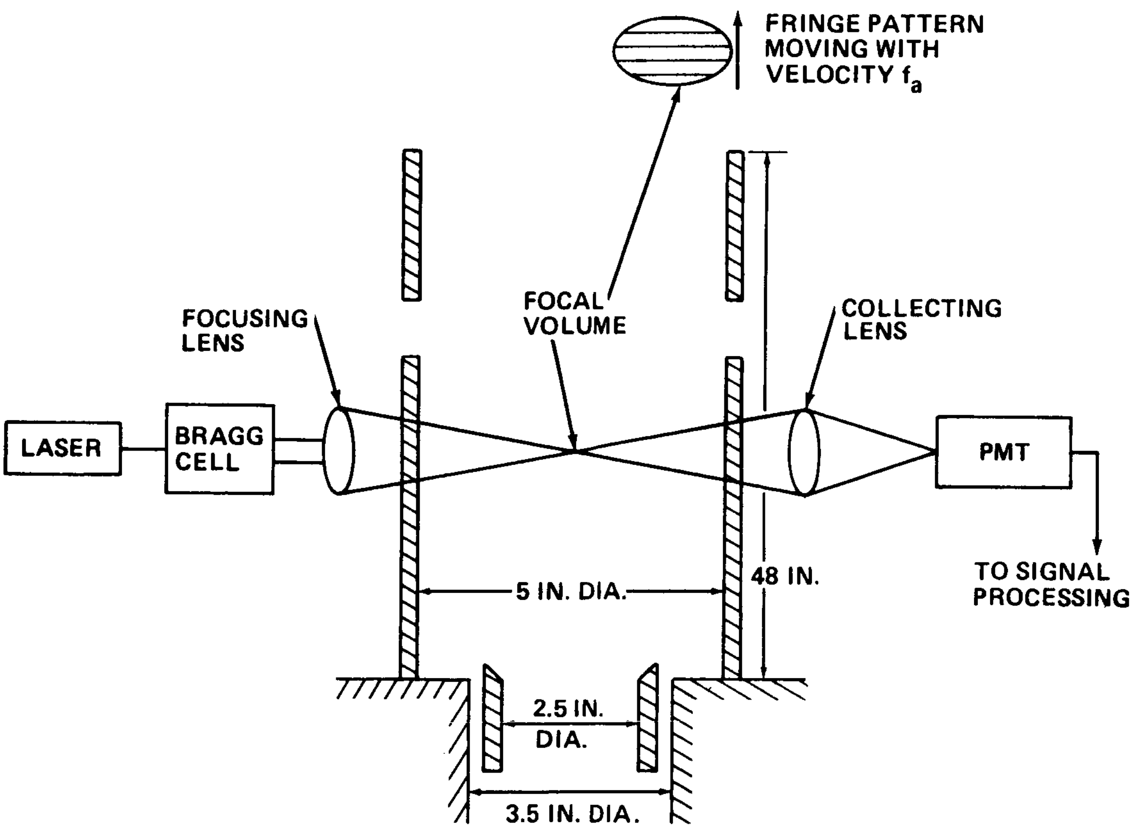

Figure 2. Schematic of the coaxial jet flow experiment of Owen [7].

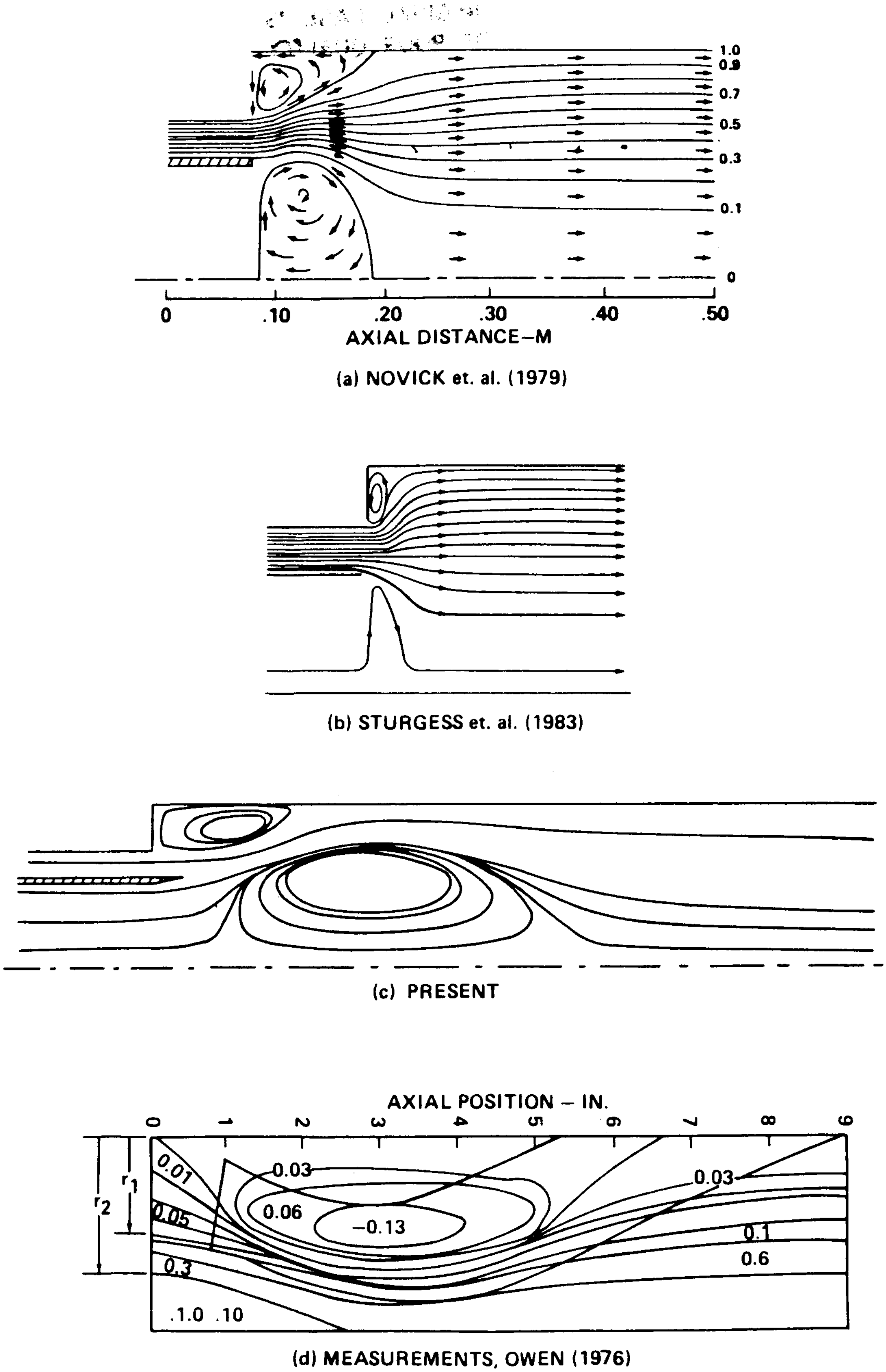

Figure 3. Predicted and measured flow patterns.

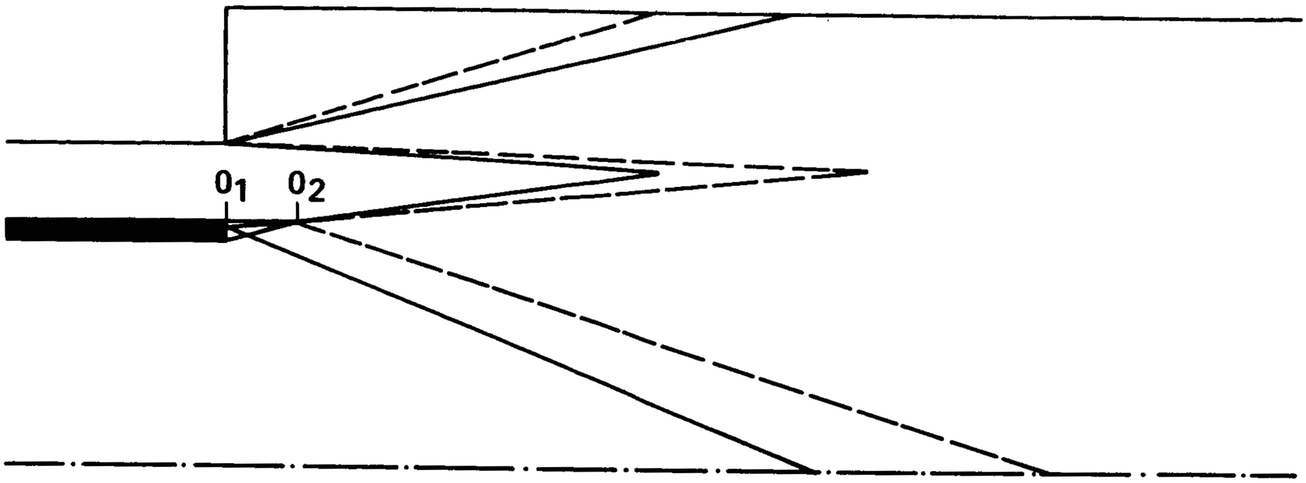

Figure 4. Growth of mixing layers — formation of recirculation zones.

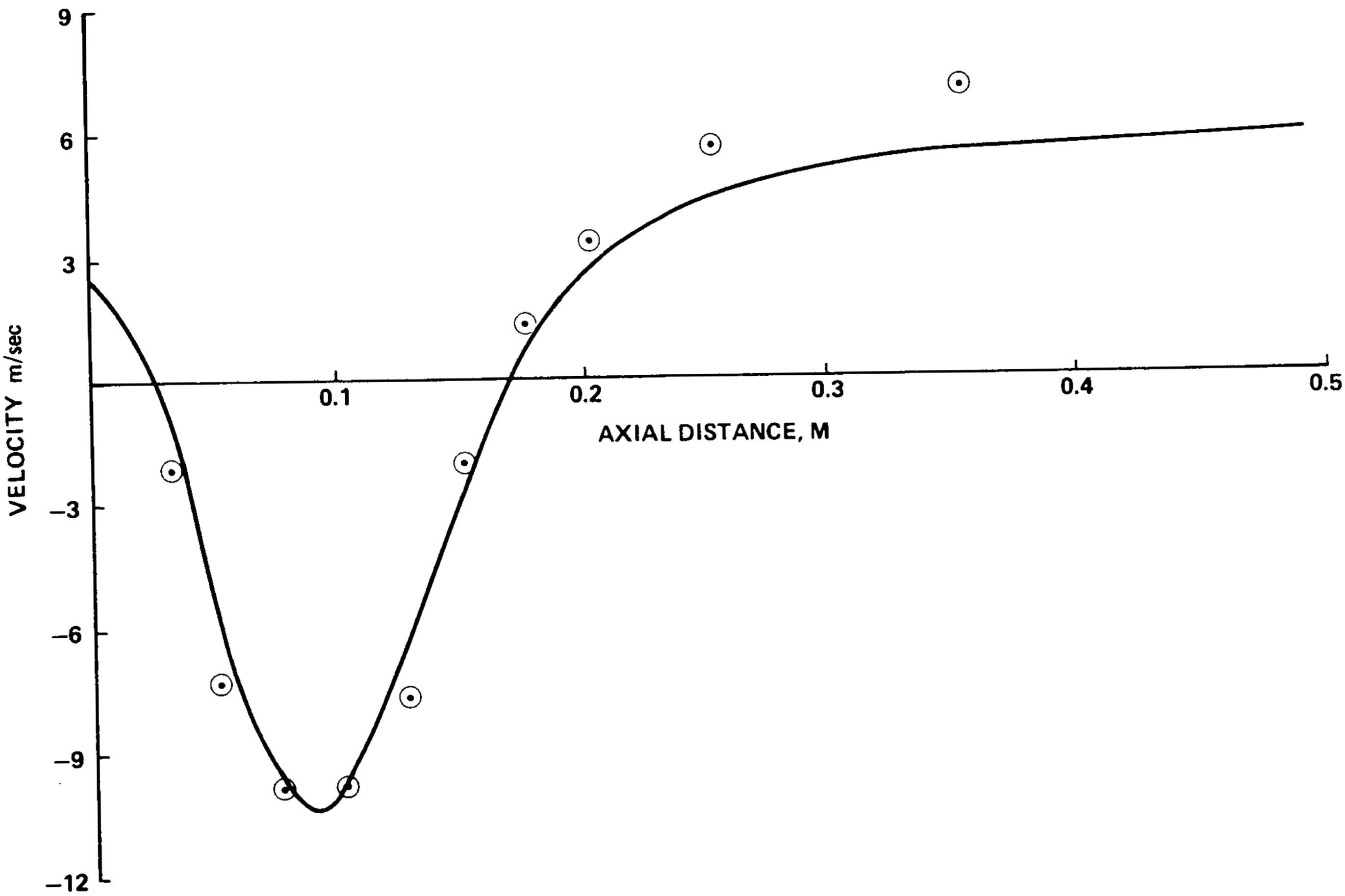

Figure 5. Axial mean velocity along the centerline.
—— prediction, ⊙ measurement [7].

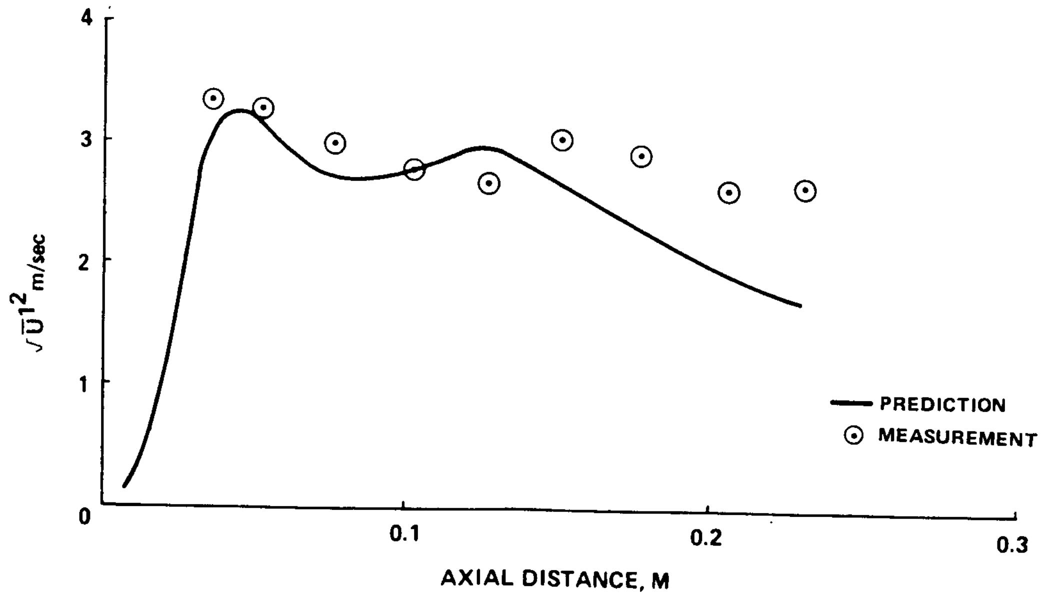

Figure 6. Axial turbulence intensity on the centerline.

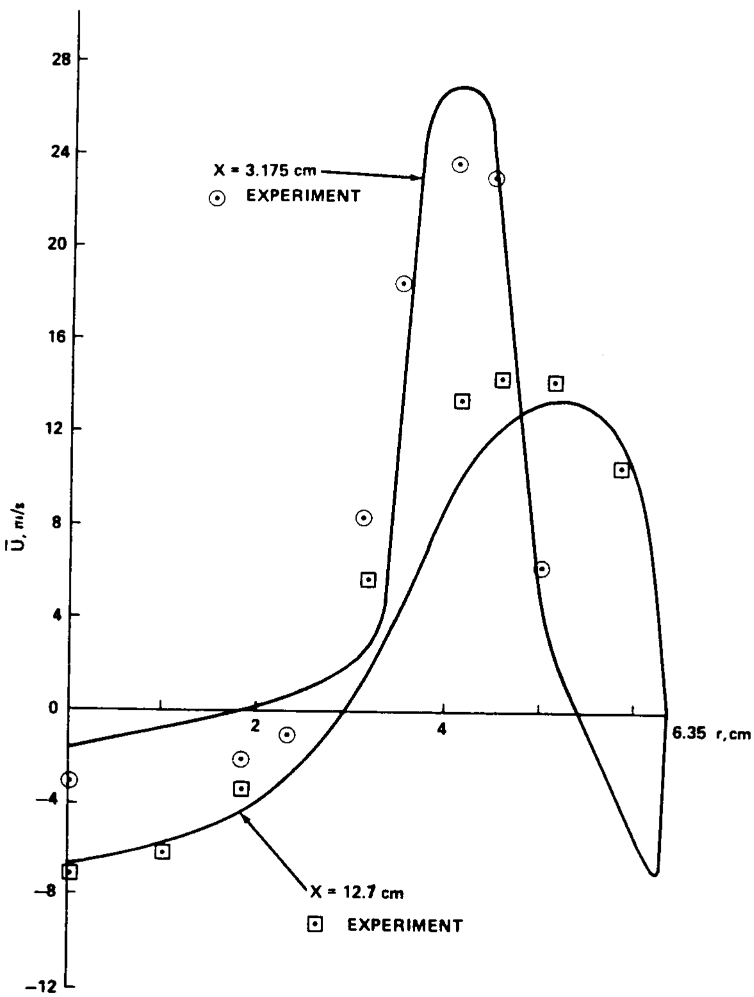

Figure 7. Mean axial velocity profiles.

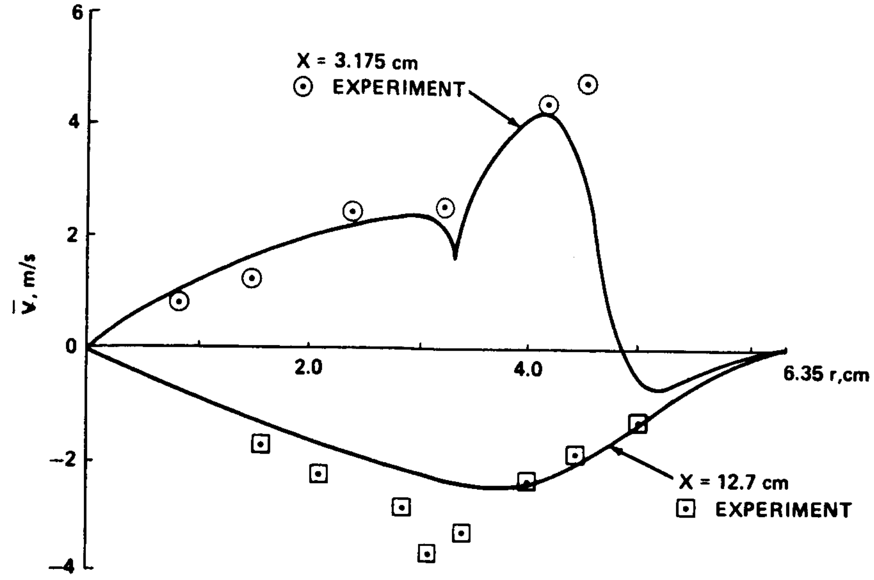

Figure 8. Mean radial velocity profiles.

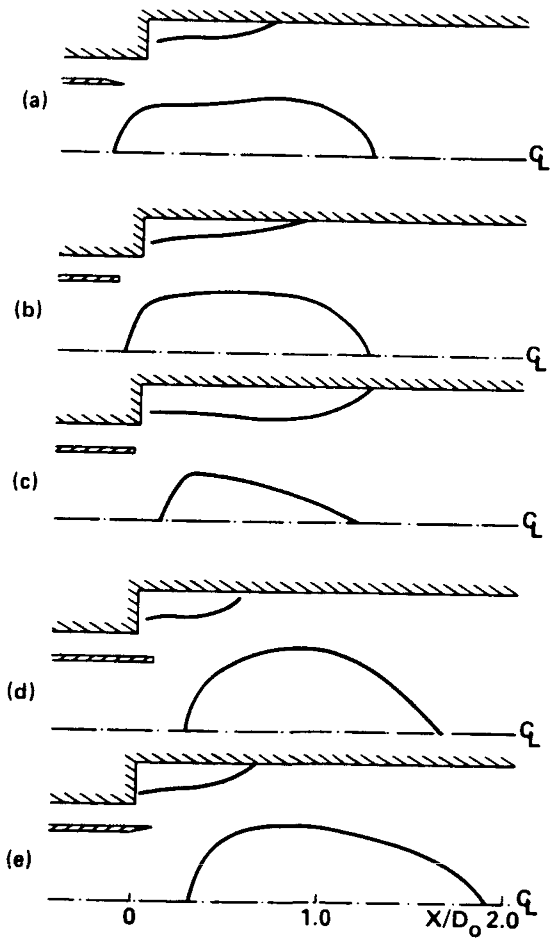

Figure 9. Variations of loci of flow reversals with central jet exit configuration.

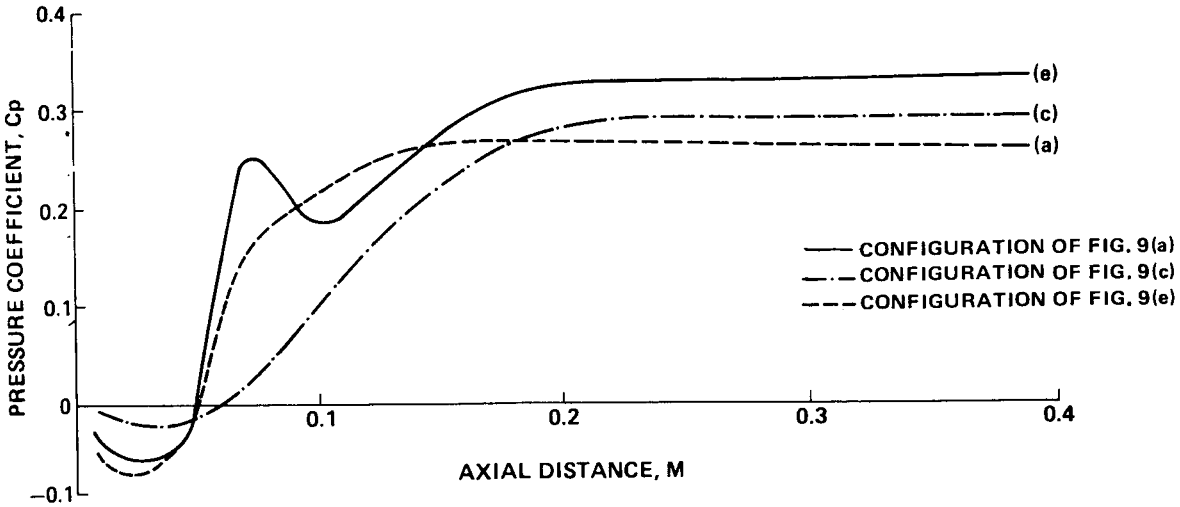

Figure 10. Computed wall static pressure.

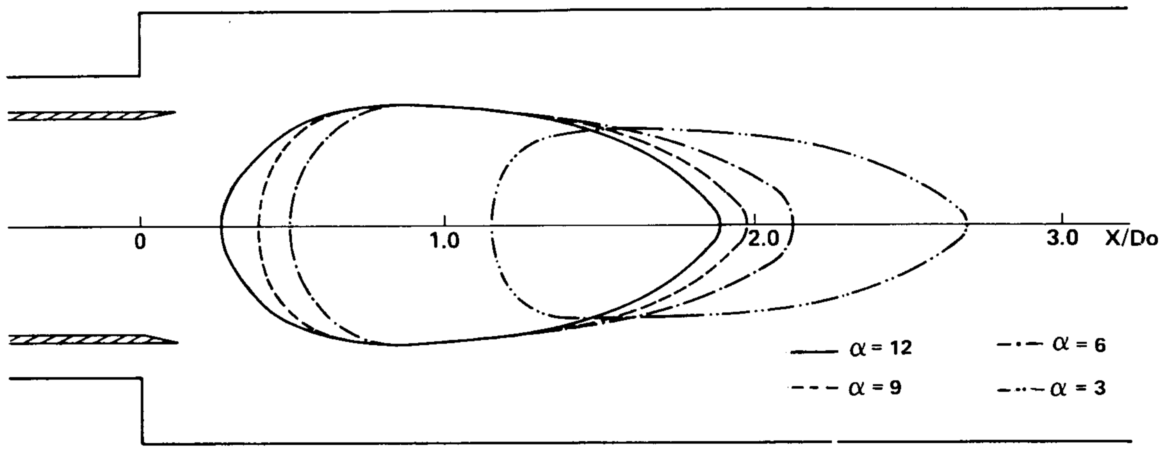

Figure 11. Effect of velocity ratio on the central toroidal recirculation zone.

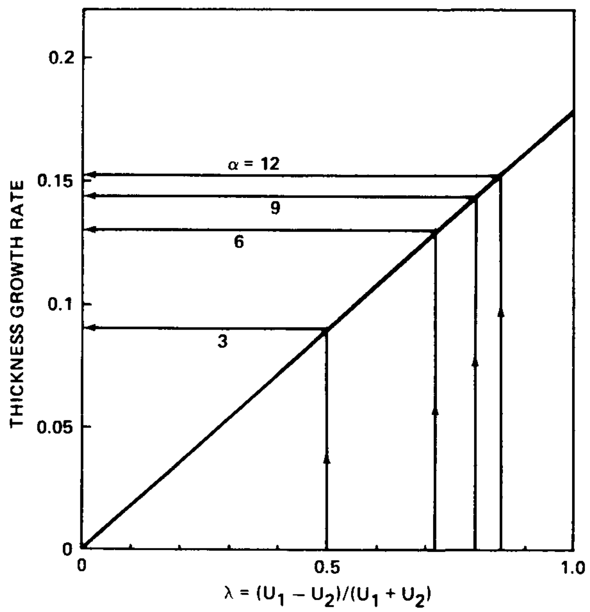

Figure 12. Mixing layer growth rate as a function of the velocity difference parameter, $\lambda \doteq (U_1 - U_2)/(U_1 + U_2)$.

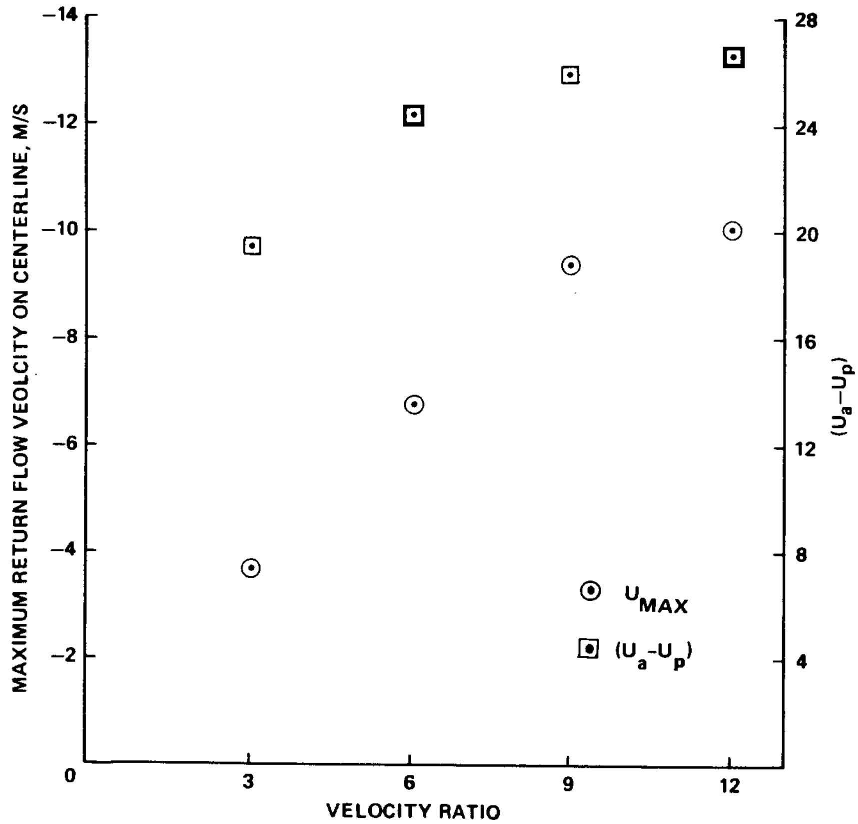

Figure 13. Effect of velocity ratio on the maximum return flow velocity in the central toroidal recirculation zone.

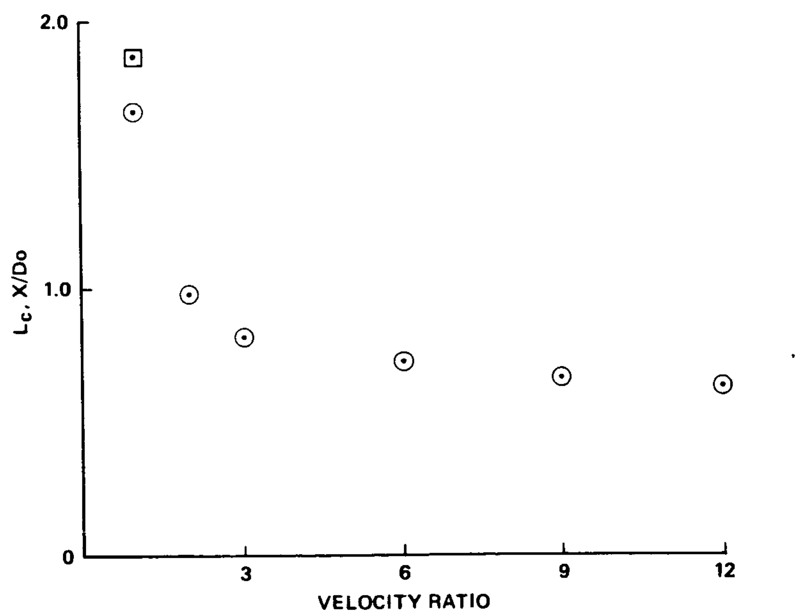

Figure 14. Effect of velocity ratio on the length of the corner recirculation zone.

1. REPORT NO.	2. GOVERNMENT ACCESSION NO.	3. RECIPIENT'S CATALOG NO.
NASA CR-4064		

4. TITLE AND SUBTITLE	5. REPORT DATE
Prediction of Recirculation Zones in Isothermal Coaxial Jet Flows Relevant to Combustors	April 1987
	6. PERFORMING ORGANIZATION CODE
7. AUTHOR(S) M. Nallasamy	8. PERFORMING ORGANIZATION REPORT #
9. PERFORMING ORGANIZATION NAME AND ADDRESS Universities Space Research Association P.O. Box 3006 Boulder, Colorado 80307	10. WORK UNIT NO. M-556
	11. CONTRACT OR GRANT NO. NAS8-35918
12. SPONSORING AGENCY NAME AND ADDRESS National Aeronautics and Space Administration Washington, D.C. 20546	13. TYPE OF REPORT & PERIOD COVERED Contractor Report
	14. SPONSORING AGENCY CODE

15. SUPPLEMENTARY NOTES Technical Monitor: N. Costes, G. Fichtl

Prepared by Earth Science and Applications Division, Structures and Dynamics Laboratory, Science and Engineering Directorate.

16. ABSTRACT

The characteristics of the recirculation zones in confined coaxial turbulent jets are investigated numerically employing the k-ε turbulence model. The geometrical arrangement corresponds to the experimental study of Owen (AIAA J. 1976) and the investigation is undertaken to provide information for isothermal flow relevant to combustor flows. For the first time, the shape, size, and location of the recirculation zones for the above experimental configuration are correctly predicted. The processes leading to the observed results are explained. Detailed comparisons of the prediction with measurements are made. It is shown that the recirculation zones are very sensitive to the central jet exit configuration and the velocity ratio of the jets.

17. KEY WORDS	18. DISTRIBUTION STATEMENT
Combustors Turbulence Model Turbulence Recirculating Flows Computational Fluid Dynamics	Unclassified — Unlimited Subject Category: 34

19. SECURITY CLASSIF. (of this report)	20. SECURITY CLASSIF. (of this page)	21. NO. OF PAGES	22. PRICE
Unclassified	Unclassified	21	A01

For sale by National Technical Information Service, Springfield, Virginia 22161

NASA-Langley, 1987